International Journal of Minerals, Metallurgy and Materials
Volume 30, Number 2, February 2023, Page 314
https://doi.org/10.1007/s12613-022-2432-5

Combustion performance of pulverized coal and corresponding kinetics study after adding the additives of Fe_2O_3 and CaO

Qiangjian Gao[1,2),✉], *Guopeng Zhang*[1,2)], *Haiyan Zheng*[1,2)], *Xin Jiang*[1,2)], *and Fengman Shen*[1,2)]

1) Key Laboratory for Ecological Metallurgy of Multimetallic Mineral (Ministry of Education), Northeastern University, Shenyang 110819, China
2) School of Metallurgy, Northeastern University, Shenyang 110819, China

(Received: 23 November 2021; revised: 26 January 2022; accepted: 29 January 2022)

Abstract: Combustion performance of pulverized coal (PC) in blast furnace (BF) process is regarded as a criteria parameter to assess the proper injection dosage of PC. In this paper, effects of two kinds of additives, Fe_2O_3 and CaO, on PC combustion were studied using the thermogravimetric method. The results demonstrate that both the Fe_2O_3 and CaO can promote combustion performance index of PC including ignition index (C_i), burnout index (D_b), as well as comprehensive combustibility index (S_n). The S_n increases from 1.37×10^{-6} to 2.16×10^{-6} $\%^2 \cdot \text{min}^{-2} \cdot {}^\circ\text{C}^{-3}$ as the Fe_2O_3 proportion increases from 0 to 5.0wt%. Additionally, the combustion kinetics of PC was clarified using the Coats-Redfern method. The results show that the activation energy (E) of PC combustion decreases after adding the above additives. For instance, the E decreases from 56.54 to 35.75 kJ/mol when the Fe_2O_3 proportion increases from 0 to 5.0wt%, which supports the improved combustion performance. Moreover, it is uneconomic to utilize pure Fe_2O_3 and CaO in production. Based on economy analysis, we selected the iron-bearing dust (IBD) which contains much Fe_2O_3 and CaO component to investigate, and got the same effects. Therefore, the IBD is a potential option for catalytic PC combustion in BF process.

Keywords: pulverized coal; combustion performance; blast furnace; kinetics; additives

1. Introduction

Blast furnace (BF) process—a vital part of steelmaking—is a traditional and efficient method to achieve continuous production of hot metal (HM) particularly at large scale and low cost [1]. The yield of HM produced by BF is accounting for >70% all over the world [2–3]. As a typical technology of BF process, the pulverized coal injection (PCI) operation has many merits in terms of economy and environmental protection [4–9]: using lower price coal to replace the expensive metallurgical coke, which is favorable for cost-saving in ironmaking; reducing coke consumption, favorable for avoiding environment pollution in coking; cooperating with oxygen enrichment operation in PCI process, favorable for enhancing the stability of BF process; higher hydrogen content of PC than coke, favorable for increasing the H_2 portion in BF, etc. Therefore, the PCI dosage per unit HM is increasing higher up to about 180 kg/t for most of BFs and even 250 kg/t for parts of BFs. However, PCI operation also has an inevitable drawback [10–12]. For instance, when the pulverized coal (PC) is injected into BF, the residence time is limited attributing the higher PC flow rate. As a result, the accumulation of unburned PC in BF is a challenging issue, which may lead to deteriorating burden permeability and restraining production efficiency of BF. In addition, the fluidity of melting slag may be negatively affected as the unburned PC goes into the slag [13]. Consequently, combustion performance and efficiency of PC are regarded as criteria parameters in PCI operation.

Many previous papers have reported to promote the combustion performance of PC by adjusting operating conditions in BF process. Kim's group [14–15] pointed out in their previous papers that combustion performance can be affected via changing the temperature and CO emission on the combustion process. Additionally, the fragmentation phenomenon is considered as a vital factor affecting the PC combustion performance. Luo *et al*. [16] studied the flow and combustion performance of PC basing on combustion experiments. The temperature distribution of gas and unburned carbon was obtained. Dacombe *et al.* [17] maintained that the coal particle combustion process is related with the particle size, temperature conditions, coal category, even content of volatile matter, etc. Friedemann *et al.* [18] described that the temperature difference between the core layer and outer layer of PC particle can result in tensile stress. The high rank coal appears few pores, which easily result in fragmentation. Similarly, Lee *et al.* [19] investigated the influence of temperature variation, coal properties, and particle size distribution on fragmentation during the devolatilization of coal combustion process. The results prove that high temperature could promote the fragmentation index. Shen *et al.* [20–21] studied the operating parameters of BF process containing temperature

---

✉ Corresponding author: Qiangjian Gao E-mail: gaoqiangjian@163.com

distribution in BF, oxygen enrichment ratio, cooling gas choice, and PCI dosage, and these operating parameters may negatively or positively affect the combustion process of PC.

Moreover, some researchers found that the issue of unburned PC accumulation in BF can be settled by adding some additives to improve the PC's combustion. It was proven that part of alkali metal, metal oxides, and metal salts, as well as rare earth metal compounds may play a positive role in improving the combustion process of coal and promoting PCI dosage to reduce the cost. Abbasi-Atibeh and Yozgatligil [22] maintained that the K-bearing catalyst appears well catalytic performance and make the burnout temperature of coal lower. But the alkali metal is also negative substances in BF process due to the alkali metal nodulation in BF. Shen *et al.* [23] reported that PCI blending with MnO_2 can accelerate the combustion of PC. However, the MnO_2 can lead to the viscosity of slag lower and then worsen the desulfurization ability of BF slag. Zhang *et al.* [24] investigated the PC combustion behavior in the condition of BF process. The results showed that the PC combustion is positively influenced after blending with $CaCO_3$ and CO_2. Li *et al.* [25] found that metal oxides of CuO and ZnO can lower the ignition temperature and speed up the combustion rate of PC. Besides, in a previous paper [26], CeO_2 (a rare earth metal oxide) was found to effectively decrease the ignition temperature of coal and promote the burnout of coal. The catalytic action of CeO_2 attributes the fact that the released oxygen from CeO_2 plays a positive role in the oxygen-lacking combustion process, which is in favor of fixed carbon's combustion and volatile matters' release in PC combustion process. But it is much uneconomical for rare earth metal oxide of CeO_2 to be utilized as a catalyst in such a large scale industry production like PCI process of BF process. Liu *et al.* [27] stated that $FeCl_3$ and $FeCl_2$ can also contribute to decline the activation energy of Tongchuan coal (China) during combustion process. It is worth mentioned that the chloride seriously corrodes the equipment and then destroy the production rhythm. In addition, some works for biomass/biomass-bearing waste combustion cases has been referred containing the individual combustion of biomass and co-combustion of biomass blending with some other additives. Liu *et al.* [28] maintained that they had obtained the product distribution of sulfur in sewage sludge combustion process after adding CaO and Fenton, and Fang *et al*. [29] mentioned in their paper that the oxides including MgO and ZnO contributed to reduce the activation energy of paper sludge combustion process.

Summarily, most of previous works were committed to promote the combustion efficient by adjusting the BF operating conditions or adding chemical catalysts in PCI process. However, it has been proven that the BF operating conditions should be always maintained at a stable level in order to obtain the smooth running of BF [21]. Also, although some coal combustion catalysts including CeO_2, MnO_2, ZnO, $FeCl_3$, as well as alkali metal compounds are effective to promote the PC combustion, the high cost and even part of them such as chloride, alkali metal compounds, and ZnO are regarded as hazardous substance in BF ironmaking process, which make them uneconomical and even risky for large-scale industrial applications during the PCI process. Thus, it is significant to find other catalysts which can catalyze the combustion of PC at large scale, minimize cost, and lower risk. It is acknowledged that Fe_2O_3 and CaO are essential elements for ironmaking [30]. Both the Fe_2O_3 and CaO are relatively low-cost, easily obtained, and indispensable components of BF process, comparing with CeO_2, MnO_2, ZnO, as well as alkali metal compounds. But in fact, the detailed role the Fe_2O_3 and CaO play in the PC combustion process is not clearly. Therefore, further research is still necessary. In this work, the effects of Fe_2O_3 and CaO on combustion process of PC were respectively studied. The kinetic parameters such as activation energy (E) and pre-exponential factor (A) were obtained via Coats-Redfern integral method to study the combustion process after blending with additives. This work aims to provide a significant guidance in aspect of PCI catalyzed combustion process.

2. Experimental

2.1. Sample preparation

A typical anthracite coal from Shanxi province of China was chosen to study the combustion behavior in the present work. Before experiments, the anthracite coal was put into an oven for drying, and then sieved in order to attain the PC powder with the portion of particle size of less than 74 μm (−74 μm) overtop 80%. The analytical reagents of Fe_2O_3 and CaO were also dried and prepared for the experiments. The corresponding ultimate analysis, low heating value analysis, as well as proximate analysis of PC listed in Table 1 was tested according the China nation standards of GB/T212-2008 [31] and GB/T213-2008 [32]. One can conclude that the volatile content is 12.09wt% and the fixed carbon content is 74.45wt%. The low heating value is 30.86 kJ/g.

The particle sizes of experimental materials analyzed using the MASTERSIZER2000 laser particle size analyzer were shown in Fig. 1. The particle sizes of three kinds of raw materials (coal, Fe_2O_3 and CaO) are suitable for the tests which require the −74 μm portion overtops 80% [33].

Table 1. Proximate analysis and ultimate analysis of coal sample

Proximate analysis (ad) / wt%				Ultimate analysis (ad) / wt%					LHV (ad) / ($kJ\cdot g^{-1}$)
M	A	V	FC	C	H	O	N	S	
2.62	10.84	12.09	74.45	77.2	3.22	3.87	1.11	0.63	30.86

Note: A, V, FC, M, LHV, and ad represent ash, volatile matters, fixed carbon, moisture, low heating value, and air dried basis, respectively.

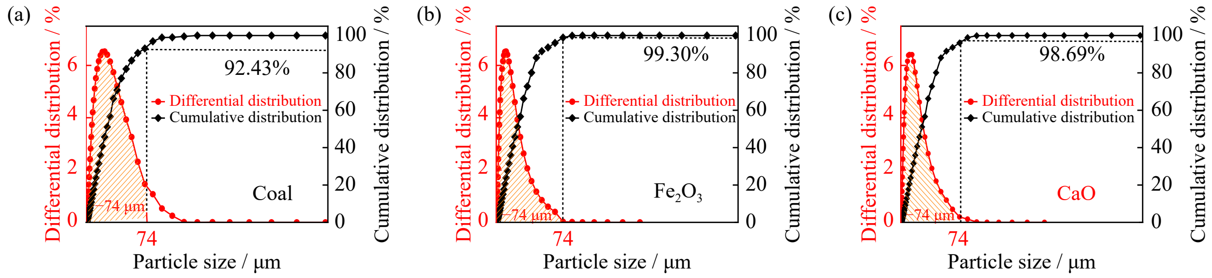

Fig. 1. Particle sizes of experimental materials: (a) coal; (b) Fe_2O_3; (c) CaO.

2.2. Methods and plans

The combustion experiments were carried out on a NETZSCHSTA449F3 thermo-gravimetric analyzer. Considering the fact that the target of PCI operation is to use adequate coal in BF process, therefore, the blending portions of additives (Fe_2O_3 and CaO) in PC were designed as 0, 2.5wt%, and 5.0wt%, respectively. The original mass of the sample was set at (20 ± 0.1) mg in our experiments. Actually, the coal combustion in BF process usually appears at air atmosphere. Therefore, in this work, the coal blends were heated from 25 to 1000°C in air atmosphere which was produced by mixing the O_2 and N_2 with the volume ratio of 1:4 as shown in Fig. 2. The flow rate was set at 100 mL/min and the heating rate was set at 15°C/min in sample heating process. For the sake of obtaining accurate results, every experimental result was confirmed according to the average of reproducibility test.

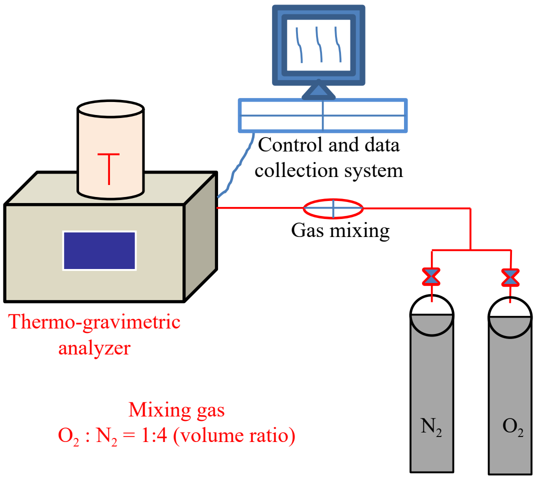

Fig. 2. Schema of thermo-gravimetric system for coal combustion.

2.3. Combustion performance and efficiency

2.3.1. Combustion performance parameter

In this work, ignition temperature (T_i), maximum mass loss rate $(\mathrm{d}w/\mathrm{d}t)_{\max}$ (w and t represent the sample mass and the combustion time, respectively), peak temperature (T_m), and burnout temperature (T_b) were adopted to assess the PC combustion behavior. The detailed determination method [34] is shown in Fig. 3.

Firstly, a vertical from the $(\mathrm{d}w/\mathrm{d}t)_{\max}$ point in derivative thermal gravimetric (DTG) profile was constructed, and it intersects the thermogravimetric (TG) curve at point *A*. Secondly, a tangent of TG curves from *A* point was drawn, and it intersects with a parallel line of *x*-axis where the mass loss is 0 (i.e., TG = 100%) at point *C*. The corresponding temperature of the *C* point is defined as ignition temperature (T_i,°C). As the mass loss stops during combustion, the temperature is defined as burnout temperature (T_b,°C). The temperature at $(\mathrm{d}w/\mathrm{d}t)_{\max}$ is defined as peak temperature (T_m,°C).

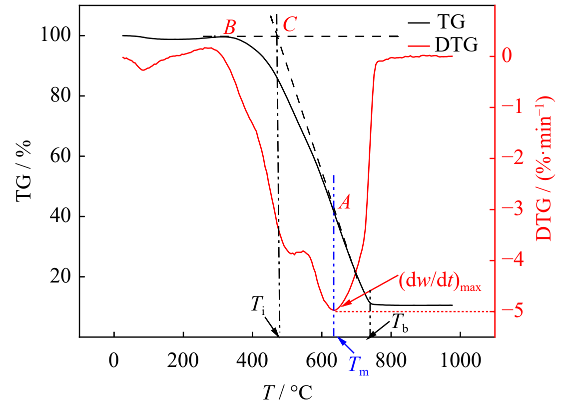

Fig. 3. Definition methods of T_i, T_b, and T_m.

Meanwhile, ignition index (C_i), burnout index (D_b), and comprehensive combustibility index (S_n) were introduced to estimate the ignition performance, burnout performance, and comprehensive combustibility performance, respectively. These parameters can be calculated basing on the previous paper [35], as presented in Eqs. (1)–(3).

Ignition index C_i (%·min^{-1}·°C^{-2}):

$$C_i = \frac{(\mathrm{d}w/\mathrm{d}t)_{\max}}{T_i^2} \tag{1}$$

Burnout index D_b (%·min^{-4}):

$$D_b = \frac{(\mathrm{d}w/\mathrm{d}t)_{\max}}{\nabla t_{1/2} \cdot t_{\max} \cdot t_b} \tag{2}$$

Comprehensive combustibility index S_n (%^{2}·min^{-2}·°C^{-3}):

$$S_n = \frac{(\mathrm{d}w/\mathrm{d}t)_{\max} \cdot (\mathrm{d}w/\mathrm{d}t)_{\mathrm{mean}}}{T_i^2 \cdot T_b} \tag{3}$$

where $(\mathrm{d}w/\mathrm{d}t)_{\max}$ represents the maximum mass loss rate (%/min); $(\mathrm{d}w/\mathrm{d}t)_{\mathrm{mean}}$ represents the average mass loss rate (%/min); t_i and t_b represent the times of attaining ignition and burnout temperatures, respectively; $t_{\max}$ represents the time of attaining peak temperature; $\Delta t_{1/2}$ represents the time as $(\mathrm{d}w/\mathrm{d}t)/(\mathrm{d}w/\mathrm{d}t)_{\max} = 1/2$.

Ignition index C_i was defined to describe the ignition performance of fuel. Higher C_i indicates the stronger reactivity in early combustion stage. Burnout index D_b was defined to describe burnout performance. The D_b value higher, the burnout performance appears better. Comprehensive combustibility index S_n was used to assess the whole combustion performance.

2.3.2. Combustion efficiency parameter

Combustion efficiency is also considered as a significant index to evaluate the PC combustion performance. The combustion efficiency can be evaluated by the heat (Q) which can be obtained basing on the differential scanning calorimetry (DSC) curves [36]. The Q value is bigger means that the combustion efficiency is higher.

$$Q = \frac{k\int h(t)\,\mathrm{d}t}{m_0(1-x)} = \frac{kS}{m_0(1-x)} \tag{4}$$

where $h(t) = f(t_1) - f(t_2)$, and $f(t)$ is the DSC profile; k is a constant; m_0 is weight of sample; x is percentage of additive in PC; S is the area enclosed by DSC curves.

$c_{\max}$ is the maximum of DSC. The larger $c_{\max}$ indicates that the burning intensity of the unit mass coal is higher.

3. Results and discussion

3.1. Individual combustion process of pulverized coal

The combustion curves of PC containing TG, DTG, and DSC are presented in Fig. 4. From the Fig. 4, there is a two stage mass loss in the DTG curves of PC. The stage I sharing about 38% mass loss of locates in 350–550°C, attributing to the decomposition of volatile matters content [37–38]. The stage II accounting for nearly 50% mass loss locates in 550–750°C, which attributes to the combustion of carbon. Look at the DTG curve, the PC combustion presents two peak points at 506°C and 611°C, and the corresponding $(\mathrm{d}w/\mathrm{d}t)_{\max}$ are 4.56%/min and 6.18%/min. The combustion performance parameters such as T_i, T_m, and T_b are 442, 611, and 741°C, respectively. The $c_{\max}$ here is 5.40 mW/mg.

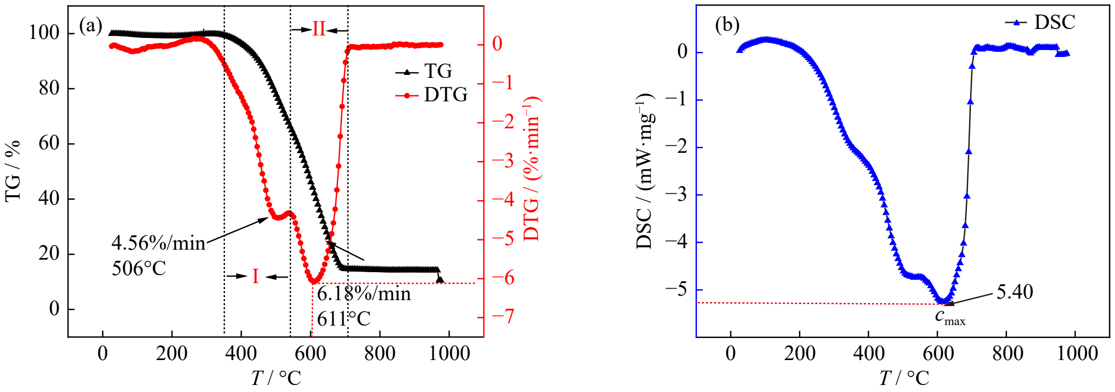

Fig. 4. TG, DTG, and DSC curves of the combustion process for single coal: (a) TG–DTG; (b) DSC.

3.2. Combustion process of pulverized coal blending with additives

3.2.1. Combustion performance parameter

The combustion process curves of PC blending with Fe_2O_3 or CaO, whose proportions are 0, 2.5wt% and 5.0wt%, are presented in Figs. 5 and 6. As shown in Fig. 5, the TG curve profiles of the PC blending with Fe_2O_3 resemble with the TG curve of single PC. But it is worth to mention that mass loss appears faster and this in turn helps the decrease of T_b from 741 to 721 and 706°C when percentage of Fe_2O_3 powder increases from 0 to 2.5wt% and 5.0wt%. Similarly, Larionov *et al.* [39] also found a shift to lower temperatures occurred in TG curve, which lead to a decrease in T_b, when they adding the additive of $Fe(NO_3)_2$ in lignite coal. Analogously, the shapes of DTG profiles have no evident changes with addition of Fe_2O_3. However, the combustion curves change to lower temperature region leading to the T_i and T_m decrease by 40 and 20°C, respectively. Larionov *et al.* [39] also stated that the T_i and T_m decrease by 77 and 41°C when they blend 5.0wt% $Fe(NO_3)_2$ additive in lignite coal. Similarly, as shown in Fig. 6, the TG–DTG curve profiles of the PC blending

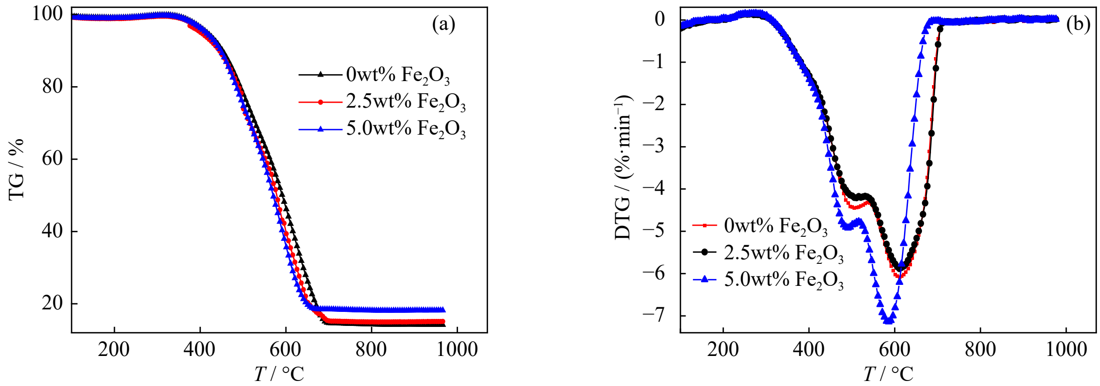

Fig. 5. TG (a) and DTG (b) curves of the combustion process for pulverized coal blending with Fe_2O_3.

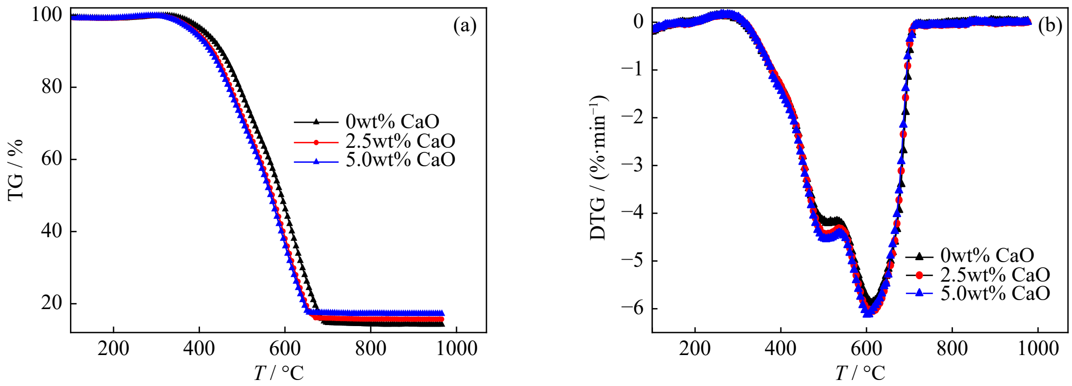

Fig. 6. TG (a) and DTG (b) curves of the combustion process for PC blending with CaO.

with CaO are also similar with single coal, and the changes of combustion parameters appear the same with the PC blending with Fe_2O_3. Adding CaO in present work also accelerates the combustion of fuel, but the catalytic effect of CaO is weaker than that of Fe_2O_3 as adding the same dosage.

The combustion parameters of PC blending with additives are listed in Table 2. Ignition temperature (T_i) and burnout temperature (T_b) rapidly reduce with increasing additives dosage of Fe_2O_3 and CaO respectively, indicating that the coal can combust ahead after adding the additives. The $(dw/dt)_{max}$ slightly increases, meaning that both the Fe_2O_3 and CaO can strength the PC combustion.

The combustion performance indexes calculated from combustion parameters are shown in Table 3. From the Table, we can attain the following findings.

(1) The ignition index of PC enhances from 3.01×10^{-5} to 4.53×10^{-5} %·min^{-1}·°C^{-2} for PC blending with Fe_2O_3 and 3.01×10^{-5} to 3.44×10^{-5} %·min^{-1}·°C^{-2} for PC blending with CaO, which signifies that the ignition performance is notably prompted with addition of the additives, and the PC can be quickly ignited in BF process. It is reported that the reaction of bond breaking for PC usually begins at least 300°C, and this stage will produce many radical fragments [36]. These radical fragments with high activity PC can help the aromatics ignition and decomposition. However, when the ignition temperature is too low, it will riskily affect the PCI process attributing to the explosion of PC [9].

(2) The burnout index of PC sharply increases from 5.8×10^{-6} to 7.8×10^{-6} %·min^{-4} for PC blending with Fe_2O_3 and 5.8×10^{-6} to 6.5×10^{-6} %·min^{-4} for PC blending with CaO as the proportion of additives varies from 0 to 5.0wt%, meanings that the PC will be easier to burnout, which is beneficent to reduce accumulation of unburned PC in BF. (3) The comprehensive combustibility index of PC improves as the additives are added into PC, signifying the comprehensive combustion performance improves gradually. Comparing with the Fe_2O_3, the CaO catalytic ability is weaker.

In summary, the PC combustion process is obviously promoted with addition of additives containing Fe_2O_3 or CaO from 0 to 5.0wt%, which indicates that the additives probably catalyze the combustion of PC. Wang *et al.* [26] interpreted that part of metal oxides can catalyze the PC combustion because the metal oxides play an important role in oxygen transfer between the carbon and metal oxides.

3.2.2. Combustion efficiency parameters

Fig. 7 shows the DSC curves of PC after blending with additives. Basing on the DSC curves, the Q and C can be obtained in Fig. 8 after using the additives of Fe_2O_3 and CaO.

Comparing with the single PC, both the Q and c_{max} enhance gradually as the additives proportion increase from 0 to

Table 2. Combustion parameters for pulverized coal blending with additives (Fe_2O_3 and CaO)

Coal sample	T_i / °C	T_m / °C	T_b / °C	t_m / min	t_b / min	$\Delta t_{1/2}$ / min	$(dw/dt)_{max}$ / (%·min^{-1})	$(dw/dt)_{mean}$ / (%·min^{-1})
Single coal	442	611	741	39.1	47.7	28.6	5.88	1.79
Coal + 2.5wt%Fe_2O_3	423	606	721	38.7	46.4	28.4	6.18	1.80
Coal + 5.0wt%Fe_2O_3	402	591	706	37.7	45.4	27.9	6.99	1.89
Coal + 2.5wt%CaO	435	610	731	39.0	47.1	28.7	6.02	1.80
Coal + 5.0wt%CaO	422	601	716	38.4	46.1	28.4	6.12	1.81

Table 3. Combustion performance of pulverized coal blending with additives

Coal sample	Ignition performance, C_i / (10^{-5} %·min^{-1}·°C^{-2})	Burnout performance, D_b / (10^{-6} %·min^{-4})	Combustibility index, S_n / (10^{-6} %^{2}·min^{-2}·°C^{-3})
Single coal	3.01	5.8	1.37
Coal + 2.5wt%Fe_2O_3	3.45	6.5	1.61
Coal + 5.0wt%Fe_2O_3	4.53	7.8	2.16
Coal + 2.5wt%CaO	3.18	6.1	1.47
Coal + 5.0wt%CaO	3.44	6.5	1.62

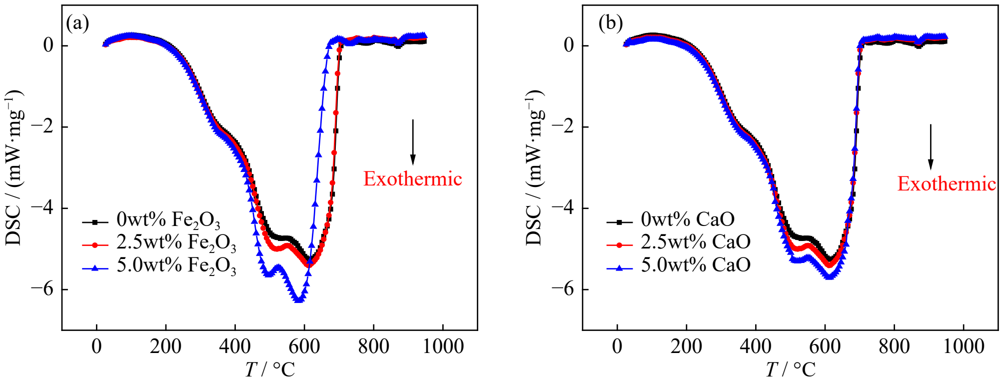

Fig. 7. DSC curves of the combustion process for pulverized coal blending with Fe_2O_3 (a) or CaO (b) additives.

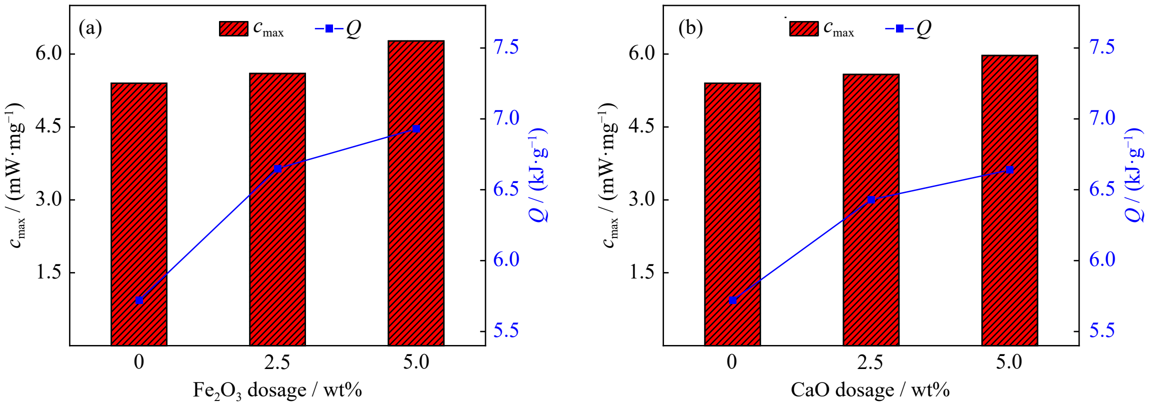

Fig. 8. Q and c_{max} for the PC blending with different proportions of Fe_2O_3 (a) or CaO (b) additives.

5.0wt%. For instances, the Q value increase from 5.72 to 6.93 kJ/g and the c_{max} value increase from 5.40 to 6.27 mW/mg with the increase Fe_2O_3 dosage from 0 to 5.0wt%. CaO presents a similar influence on combustion efficiency. These results prove that both the Fe_2O_3 and CaO can effectively enhance the combustion efficiency. The catalytic effect of additives mentioned here is obvious.

3.3. Kinetics of co-combustion of pulverized coal blending with additives

In this work, the Coats-Redfern integral method was applied to analyze the combustion kinetic of the PC [26,37, 39–40]. Generally, the conversion ratio α can be listed as Eq. (5):

$$\frac{d\alpha}{dt} = k(T)\cdot f(\alpha) \tag{5}$$

where $f(\alpha)$ is a mechanism function, and it can be described as $f(\alpha) = (1-\alpha)^n$, here n represents reaction order.

Furthermore, the combustion conversion ratio α is also defined as Eq. (6):

$$\alpha = \frac{m_1 - m_t}{m_0 - m_b} \tag{6}$$

where m_1, m_t, and m_b represent the original weight, weight at time t, and final weight of the sample, respectively.

$k(T)$, the rate constant, can be obtained by Arrhenius equation:

$$k(T) = A\exp\left(-\frac{E}{RT}\right) \tag{7}$$

where T represents temperature (K), E represents activation energy (kJ/mol), A represents pre-exponential factor (min^{-1}), and R represents universal gas constant (8.314 J·mol^{-1}·K^{-1}).

In this work, heating rate (β) is constant (15 K/min). Therefore, the β is described as Eq. (8).

$$\frac{dT}{dt} = \beta = 15 \tag{8}$$

Eq. (9) can be obtained by combined Eqs. (5) and (7).

$$\frac{d\alpha}{dt} = A\exp\left(-\frac{E}{RT}\right)(1-\alpha)^n \tag{9}$$

Eq. (10) can be obtained by combined Eqs. (8) and (9):

$$\frac{d\alpha}{(1-\alpha)^n} = \frac{A}{\beta}\exp\left(-\frac{E}{RT}\right)dT \tag{10}$$

Integrating Eq. (10) can obtain Eqs. (11) and (12).

$$\ln\left[\frac{-\ln(1-\alpha)}{T^2}\right] = \ln\left[\frac{AR}{\beta E}\left(1-\frac{2RT}{E}\right)\right] - \frac{E}{RT} \quad (n=1) \tag{11}$$

$$\ln\left[\frac{-\ln(1-\alpha)^{1-n}}{T^2}\right] = \ln\left[\frac{AR}{\beta E}\left(1-\frac{2RT}{E}\right)\right] - \frac{E}{RT} \quad (n\neq 1) \tag{12}$$

About the combustion process of fuel, the (E/RT) >> 1, and then the $(1-2RT/E) \approx 1$, therefore, the Eqs. (11) and (12) can be simplified to the following Eqs. (13) and (14):

$$\ln\left[\frac{-\ln(1-\alpha)}{T^2}\right] = \ln\frac{AR}{\beta E} - \frac{E}{RT} \quad (n=1) \tag{13}$$

$$\ln\left[\frac{-\ln(1-\alpha)^{1-n}}{T^2}\right] = \ln\frac{AR}{\beta E} - \frac{E}{RT} \quad (n\neq 1) \tag{14}$$

Finally, the activation energy E as well as pre-exponential factor A could be respectively attained according to intercept and slope of the regression line of Eqs. (13) and (14).

The kinetic of combustion process was carried out in corresponding temperature range between ignition temperature T_i and burnout temperature T_b. The activation energy (E) was used to mathematically analyze kinetic process and assess detailed influence of additives dosage on combustion process of PC.

The fitting profile of the PC blending with additives is presented in Fig. 9 by trying with different reaction orders (n).

Basing on the slope of Arrhenius plots and the highest value of R^2, we can obtain the E as shown in Table 4. One can conclude that the values of R^2 for every case appear larger than 0.99, so it is proven the results are reliable. The E of single coal, coal + 2.5wt%Fe_2O_3, and coal + 5.0wt%Fe_2O_3 are 56.54, 43.23, and 35.75 kJ/mol, respectively. Also, the E decrease from 56.54 to 49.88 kJ/mol as the CaO proportion is added from 0 to 5.0wt%. The addition of Fe_2O_3 and CaO can decline the E values during PC combustion. These findings precisely support that the combustion performance is promoted after adding the additives of Fe_2O_3 or CaO in PC (listed as Table 3).

It is found that the additives mentioned in the present work can promote the combustion activity and accelerate fixed car-

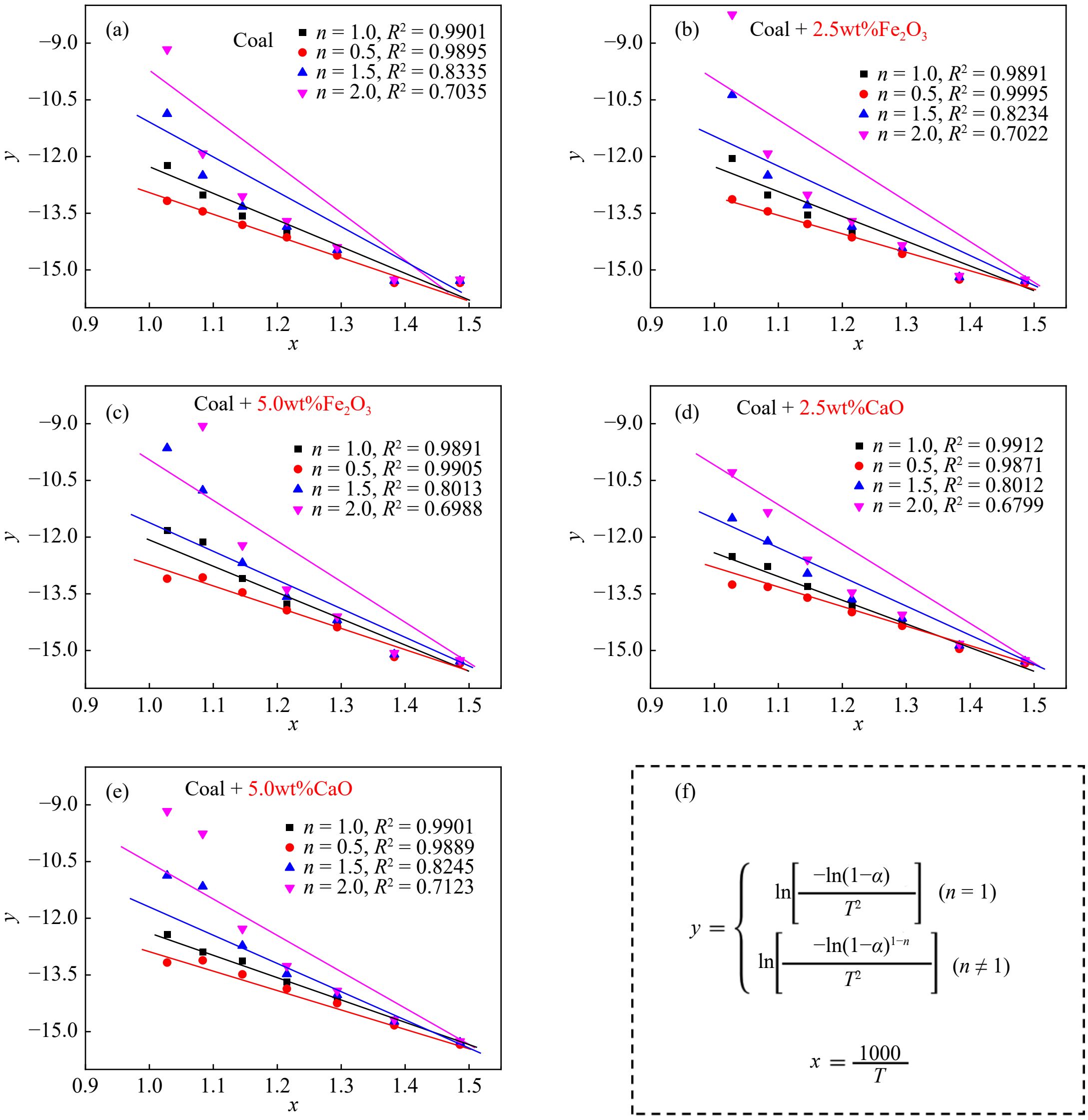

Fig. 9. Fitting profile of coal blending with additives basing on Coats-Redfern integral method: (a) coal; (b) coal + 2.5wt%Fe_2O_3; (c) coal + 5.0wt%Fe_2O_3; (d) coal + 2.5wt%CaO; (e) coal + 5.0wt%CaO; (f) Note.

Table 4. Kinetic parameters of pulverized coal blending with additives

Coal sample	T / °C	R^2	n	E / (kJ·mol^{-1})	ln A
Coal	442–741	0.9901	1	56.54	0.88
Coal + 2.5wt%Fe_2O_3	423–721	0.9995	0.5	43.23	3.14
Coal + 5.0wt%Fe_2O_3	422–706	0.9905	0.5	35.75	5.43
Coal + 2.5wt%CaO	435–731	0.9912	1	52.38	1.45
Coal + 5.0wt%CaO	422–716	0.9901	1	49.88	2.50

bon combustion. Also, the addition of additives (Fe_2O_3 and CaO) can reduce the E value in the PC combustion process. Larionov *et al.* [39] also found that the E value could decrease as blended with 5.0wt% $Fe(NO_3)_2$ in lignite attributing to the $Fe(NO_3)_2$ can decompose into Fe_2O_3 in coal combustion process. Accompanied with coal combustion, the pyrolysis is synchronously bringing out and produces much reducing gas. And the Fe_2O_3 can be reduced by the reducing gas to FeO in the condition of oxygen-lacking and contributes to the volatile matters combustion [40–41]. The FeO who is reduced from Fe_2O_3 will be oxidized again to Fe_2O_3 as the oxygen exists in atmosphere. Thus, the reduced reaction and oxidized reaction reciprocating process is to actually transfer the oxygen into the fixed carbon. Also, Fe^{3+} belong transition metal ions possessing empty orbital, which has an ability to absorb the unshared electrons. The situation mentioned above can decrease the bridged bond binding force of PC due to the presence of the electronic effect, and help to promote the volatiles release and transfer the oxygen to the surface of fixed carbon [42–44].

Guan *et al.* [45] and Cheng *et al.* [46] reported that the sulfur in PC is oxidized to gas phase due to the organic sulfur decomposition. The sulfur content is 0.63wt% in our work, (as shown in Table 1). CaO could react with sulfur and form CaS. So CaO can decrease sulfur shifting to gas phase. Thus the reaction between CaO and sulfur will reduce the consumption of oxygen in sulfur oxidation process and improve the oxygen reaction with fixed carbon, which therefore promote the combustion performance of PC. Some previous paper also [47–48] pointed out that high activity CaO can adsorb O_2 in the atmosphere and releases oxygen with high activity, then the PC reacts with active oxygen to accelerate the combustion of carbon.

3.4. Combustion process of pulverized coal blending with IBD containing Fe_2O_3 and CaO

Actually, the pure reagents of Fe_2O_3 and CaO are uneconomical to be utilized in PCI process. Thus, based on the catalytic effect of Fe_2O_3 and CaO obtained this work, a solid waste named iron-bearing dust (IBD) was selected as an alternative candidate for following reasons [49]. (1) The IBD contain the components of Fe_2O_3 and CaO which have catalytic effects proved by this paper. (2) If the IBD can replace pure Fe_2O_3 and CaO to achieve the industry catalytic effects, a lower cost will be anticipated. (3) The injecting the PC blending with IBD into BF is also helpful to dispose the solid waste IBD. Therefore, the combustion behaviors of PC, IBD and their blends were subsequently analyzed.

The chemical composition of IBD is listed in Table 5. The total Fe (TFe) content is 55.90wt% and the CaO content is 3.92wt%. Also, some other components (MgO, SiO_2, and Al_2O_3), which can be utilized for slagging process in BF, are discovered.

Table 5. Chemical composition of IBD wt%

TFe	FeO	SiO_2	CaO	MgO	Al_2O_3	C	S	Cl	Zn	Na	K
55.90	5.30	5.31	3.92	0.71	2.95	4.47	0.38	0.10	0.041	0.066	0.16

The particle size of IBD was analyzed, as shown in Fig. 10. The −74 μm portion of IBD is 93.55%. The particle size of IBD is also suitable for these tests which require the −74 μm portion overtops 80%.

For the sake of obtain the minerals composition of the IBD mentioned here, the XRD analysis was conducted. XRD pattern is presented in Fig. 11. The minerals composition of IBD mainly contains hematite (Fe_2O_3) and calcium iron olivine ($CaFeSi_2O_6$).

In the thermo-gravimetric experimental of PC blending with IBD, the portion of IBD was set as 0, 3.0wt%, and 6.0wt%. TG and DTG curves are presented in Fig. 12. From Fig. 12, one can conclude that: (1) In the TG profiles, the weight loss rate increases with addition of IBD and this in turn helps T_b decreases gradually. Moreover, the curves transfer to lower temperature region leading to the T_i and T_m decline gradually. (2) The shapes of DTG profiles have some changes with addition of IBD. These results well support the improved combustion performance after adding additives of Fe_2O_3 and CaO. Therefore, it is available and more economical to adding IBD powder to promote the PC combustion.

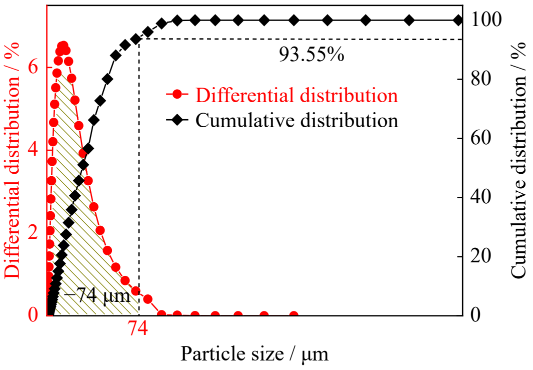

Fig. 10. Particle size of IBD.

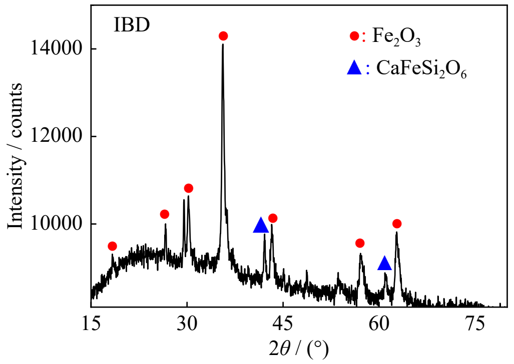

Fig. 11. XRD pattern of IBD.

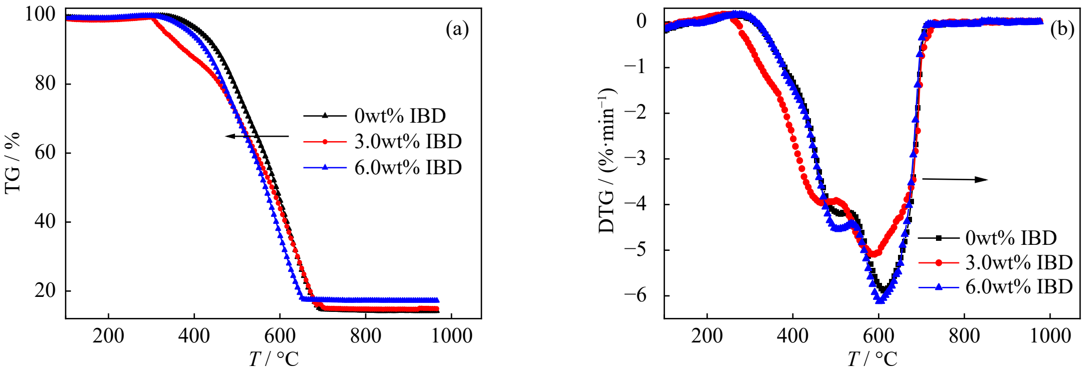

Fig. 12. TG (a) and DTG (b) curves of pulverized coal blending with IBD.

4. Conclusions

The combustion process of PC blending with additives including Fe_2O_3 and CaO were studied. Then the kinetic model was established to clarify the kinetic mechanism of the combustion. The primary findings can be collected as follows.

(1) Both the Fe_2O_3 and CaO can improve the PC combustion. The ignition temperature and burnout temperature of the PC reduce markedly as the mass percentage of additives increase from 0 to 2.5wt% and 5.0wt%, which indicates that blending with the additives can accelerate the combustion of PC.

(2) Comprehensive combustibility index (S_n), ignition index (C_i) as well as burnout index (D_b) were adopted to assess the combustion performance. Correspondingly, C_i, D_b, and S_n of the PC improve with the addition of additives. When the additive dosage increases from 0 to 5.0wt%, the values of S_n for PC increase from 1.37×10^{-6} to 2.16×10^{-6} $\%^2 \cdot min^{-2} \cdot °C^{-3}$ for Fe_2O_3 additive and from 1.37×10^{-6} to 1.62×10^{-6} $\%^2 \cdot min^{-2} \cdot °C^{-3}$ for CaO additive, respectively, which means that the comprehensive combustion performance promotes gradually and the PC tends to combust quickly in BF process.

(3) The use of additives containing Fe_2O_3 and CaO in PC obviously reduces the activation energy (E) during PC combustion process. These findings also can accurately support the fact that the combustion performance of the PC blending with additives is improved. Both the Fe_2O_3 and CaO are the potential catalysts for PC combustion.

(4) The IBD is a better substitute for catalytic combustion attributing that it contains Fe_2O_3 and CaO component. Moreover, PC blending with IBD is helpful to dispose the IBD. This method not only contributes BF necessary substances, but also promotes the combustion of fuel, and then helps to reduce accumulation of unburned PC in BF process.

Acknowledgements

This work was financially supported by the National Natural Science Foundation of China (Nos. 52074086, 51974073, 52074072, and 52074074), the Fundamental Research Funds for the Central Universities, China (No. N2225039), and the Liaoning Provincial Natural Science Foundation of China (No. 2019-MS-132).

Conflict of Interest

The authors declare that they have no known competing financial interests or personal relationships that could have appeared to influence the work reported in this paper.

References

[1] Q.J. Gao, F.M. Shen, X. Jiang, G. Wei, and H.Y. Zheng, Gas-solid reduction kinetic model of MgO-fluxed pellets, *Int. J. Miner. Metall. Mater.*, 21(2014), No. 1, p. 12.

[2] J.H. Liao, A.B. Yu, and Y.S. Shen, Modelling the injection of upgraded brown coals in an ironmaking blast furnace, *Powder Technol.*, 314(2017), p. 550.

[3] F.M. Shen, Q.J. Gao, X. Jiang, G. Wei, and H.Y. Zheng, Effect of magnesia on the compressive strength of pellets, *Int. J. Miner. Metall. Mater.*, 21(2014), No. 5, p. 431.

[4] J.G. Mathieson, J.S. Truelove, and H. Rogers, Toward an understanding of coal combustion in blast furnace tuyere injection, *Fuel*, 84(2005), No. 10, p. 1229.

[5] L.Z. Jin and X.M. Niu, Micromorphology and safety properties of meager and meager-lean coal for blast furnace injection, *Int. J. Miner. Metall. Mater.*, 28(2021), No. 5, p. 774.

[6] D.L. Wu, P. Zhou, H.J. Yan, P.Y. Shi, and C.Q. Zhou, Numerical investigation of the effects of size segregation on pulverized coal combustion in a blast furnace, *Powder Technol.*, 342(2019), p. 41.

[7] C. Wang, J.L. Zhang, G.W. Wang, K.X. Jiao, Z.J. Liu, and K.C. Chou, Combustion characteristics and kinetics of anthracite with added chlorine, *Int. J. Miner. Metall. Mater.*, 24(2017), No. 7, p. 745.

[8] Y.Q. Li, X.H. Zhang, J.Y. Zhang, J.M. Zhou, and H.J. Yan, Numerical simulation and optimization of pulverized coal injection with enriched oxygen into blast furnace, *Appl. Therm. Eng.*, 67(2014), No. 1-2, p. 72.

[9] D.W. Xiang, F.M. Shen, J.L. Yang, *et al.*, Combustion characteristics of unburned pulverized coal and its reaction kinetics with CO_2, *Int. J. Miner. Metall. Mater.*, 26(2019), No. 7, p. 811.

[10] J.A. de Castro, G.D.M. Araújo, I.D.O. da Mota, Y. Sasaki, and J.I. Yagi, Analysis of the combined injection of pulverized coal and charcoal into large blast furnaces, *J. Mater. Res. Technol.*, 2(2013), No. 4, p. 308.

[11] H.B. Zhu, W.L. Zhan, Z.J. He, Y.C. Yu, Q.H. Pang, and J.H. Zhang, Pore structure evolution during the coke graphitization process in a blast furnace, *Int. J. Miner. Metall. Mater.*, 27(2020), No. 9, p. 1226.

[12] H.B. Jiang, J.L. Zhang, J.X. Fu, J. Chang, and J. Li, Properties and structural optimization of pulverized coal for blast furnace injection, *J. Iron Steel Res. Int.*, 18(2011), No. 3, p. 6.

[13] D.W. Xiang, F.M. Shen, X. Jiang, J.L. Yang, X.J. Li, and Q.J.

Gao, Protective mechanism of unburned pulverized coal to coke in blast furnace, *J. Min. Metall. Sect. B*, 55(2019), No. 3, p. 371.

[14] J.H. Kim, R.G. Kim, G.B. Kim, and C.H. Jeon, Effect of coal fragmentation on PCI combustion zone in blast furnace, *Exp. Therm. Fluid Sci.*, 79(2016), p. 266.

[15] R.G. Kim, D.F. Li, and C.H. Jeon, Experimental investigation of ignition behavior for coal rank using a flat flame burner at a high heating rate, *Exp. Therm. Fluid Sci.*, 54(2014), p. 212.

[16] R. Luo, Y.F. Zhang, N. Li, Q.L. Zhou, and P. Sun, Experimental study on flow and combustion characteristic of a novel swirling burner based on dual register structure for pulverized coal combustion, *Exp. Therm. Fluid Sci.*, 54(2014), p. 136.

[17] P. Dacombe, M. Pourkashanian, A. Williams, and L. Yap, Combustion-induced fragmentation behavior of isolated coal particles, *Fuel*, 78(1999), No. 15, p. 1847.

[18] J. Friedemann, A. Wagner, A. Heinze, S. Krzack, and B. Meyer, Direct optical observation of coal particle fragmentation behavior in a drop-tube reactor, *Fuel*, 166(2016), p. 382.

[19] S.H. Lee, S.D. Kim, and D.H. Lee, Particle size reduction of anthracite coals during devolatilization in a thermobalance reactor, *Fuel*, 81(2002), No. 13, p. 1633.

[20] Y.S. Shen, D. Maldonado, B.Y. Guo, A.B. Yu, P. Austin, and P. Zulli, Computational fluid dynamics study of pulverized coal combustion in blast furnace raceway, *Ind. Eng. Chem. Res.*, 48(2009), No. 23, p. 10314.

[21] Y.S. Shen, B.Y. Guo, A.B. Yu, and P. Zulli, Model study of the effects of coal properties and blast conditions on pulverized coal combustion, *ISIJ Int.*, 49(2009), No. 6, p. 819.

[22] E. Abbasi-Atibeh and A. Yozgatligil, A study on the effects of catalysts on pyrolysis and combustion characteristics of Turkish lignite in oxy-fuel conditions, *Fuel*, 115(2014), p. 841.

[23] F. Shen, X. Peng, and Q. Zhao. The effect of MnO_2 on the combustion-supporting efficiency of Pulverized coal and its mechanism, *Iron Steel*, 33(1998), No. 9, p. 1.

[24] J.L. Zhang, G.W. Wang, J.G. Shao, Y.X. Chen, and T.J. Yang, Pulverized coal combustion of nitrogen free blast furnace, *J. Iron Steel Res. Int.*, 20(2013), No. 3, p. 1.

[25] X.G. Li, B.G. Ma, L. Xu, Z.T. Luo, and K. Wang, Catalytic effect of metallic oxides on combustion behavior of high ash coal, *Energy Fuels*, 21(2007), No. 5, p. 2669.

[26] Z.Q. Wang, C. Hong, Y. Xing, Y.F. Li, L.H. Feng, and M.M. Jia, Combustion behaviors and kinetics of sewage sludge blended with pulverized coal: With and without catalysts, *Waste Manage.*, 74(2018), p. 288.

[27] Y.H. Liu, D.F. Che, Y.T. Li, Effect of iron compounds on coal combustion characteristics, *J. Xi'an Jiaotong Univ.*, 34(2000), No. 9, p. 20.

[28] H. Liu, Q. Zhang, H.X. Xing, H.Y. Hu, A.J. Li, and H. Yao, Product distribution and sulfur behavior in sewage sludge pyrolysis: Synergistic effect of Fenton peroxidation and CaO conditioning, *Fuel*, 159(2015), p. 68.

[29] S.W. Fang, Z.S. Yu, Y. Lin, *et al.*, Effects of additives on the co-pyrolysis of municipal solid waste and paper sludge by using thermogravimetric analysis, *Bioresour. Technol.*, 209(2016), p. 265.

[30] F.M. Shen, B. Sundelin, K. Paulsson, *et al.*, Industrial practice of BiPCI process of pulverized coal injection for blast furnace ironmaking at SSAB, *Steel Res. Int.*, 79(2008), No. 1, p. 11.

[31] General Administration of Quality Supervision, Inspection and Quarantine of the People's Republic of China, and Standardization Administration of the People's Republic of China, GB/T212-2008: *Proximate Analysis of Coal*, Standards Press of China, Beijing, 2008.

[32] General Administration of Quality Supervision, Inspection and Quarantine of the People's Republic of China, and Standardization Administration of the People's Republic of China, GB/T213-2008: *Determination of Calorific Value of Coal*, Beijing, 2008.

[33] R.L. Carr, Evaluating flow properties of solids, *Chem. Eng. J.*, 72(1965), No. 2, p. 163.

[34] X.G. Li, Y. Lv, B.G. Ma, S.W. Jian, and H.B. Tan, Thermogravimetric investigation on co-combustion characteristics of tobacco residue and high-ash anthracite coal, *Bioresour. Technol.*, 102(2011), No. 20, p. 9783.

[35] Y.S. Lin, X.Q. Ma, X.X. Ning, and Z.S. Yu, TGA-FTIR analysis of co-combustion characteristics of paper sludge and oil-palm solid wastes, *Energy Convers. Manage.*, 89(2015), p. 727.

[36] G.W. Wang, J.L. Zhang, J.G. Shao, *et al.*, Thermal behavior and kinetic analysis of co-combustion of waste biomass/low rank coal blends, *Energy Convers. Manage.*, 124(2016), p. 414.

[37] S.S.J. Warne, Thermal analysis and coal assessment: An overview with new developments, *Thermochim. Acta*, 272(1996), p. 1.

[38] G.R. Liu, H.J. Song, and J.H. Wu, Thermogravimetric study and kinetic analysis of dried industrial sludge pyrolysis, *Waste Manage.*, 41(2015), p. 128.

[39] K.B. Larionov, I.V. Mishakov, K.V. Slyusarskii, V.E. Gubin, and A.A. Vedyagin, Intensification of the oxidation of lignite and coal by an activating additive of $Fe(NO_3)_2$, *Solid Fuel Chem.*, 53(2019), No. 5, p. 262.

[40] C. Zou, L. Zhang, S.Y. Cao, and C.G. Zheng, A study of combustion characteristics of pulverized coal in O_2/H_2O atmosphere, *Fuel*, 115(2014), p. 312.

[41] Y.N. Bai, J.L. Zhang, B.X. Su, H.W. Guo, and B.J. Yan, Kinetics study of Fe_2O_3 catalyzing pulverized coal combustion, *J. Iron Steel Res.*, 25(2013), No. 6, p. 8.

[42] X.Z. Gong, Z.C. Guo, and Z. Wang, Reactivity of pulverized coals during combustion catalyzed by CeO_2 and Fe_2O_3, *Combust. Flame*, 157(2010), No. 2, p. 351.

[43] C. Zou, L.Y. Wen, S.F. Zhang, C.G. Bai, and G.L. Yin, Evaluation of catalytic combustion of pulverized coal for use in pulverized coal injection (PCI) and its influence on properties of unburnt chars, *Fuel Process. Technol.*, 119(2014), p. 136.

[44] M.Y. Kou, H.B. Zuo, X.J. Ning, G.W. Wang, Z.B. Hong, H.F. Xu, and S.L. Wu, Thermogravimetric study on gasification kinetics of hydropyrolysis char derived from low rank coal, *Energy*, 188(2019), art. No. 116030.

[45] R.G. Guan, W. Li, and B.Q. Li, Effects of Ca-based additives on desulfurization during coal pyrolysis, *Fuel*, 82(2003), No. 15-17, p. 1961.

[46] S. Cheng, Y.H. Wang, N.B. Gao, F. Takahashi, A.M. Li, and K. Yoshikawa, Pyrolysis of oil sludge with oil sludge ash additive employing a stirred tank reactor, *J. Anal. Appl. Pyrolysis*, 120(2016), p. 511.

[47] X.X. Wu and L.R. Radovic, Catalytic oxidation of carbon/carbon composite materials in the presence of potassium and calcium acetates, *Carbon*, 43(2005), No. 2, p. 333.

[48] Z.G. Zhang, T. Kyotani, and A. Tomita, Dynamic behavior of surface oxygen complexes during oxygen-chemisorption and subsequent temperature-programmed desorption of calcium-loaded coal chars, *Energy Fuels*, 3(1989), No. 5, p. 566.

[49] J.X. Zhang, S.X. Liu, F.S. Niu, and Z.S. Xu, Reviews on the comprehensive utilization of metallurgical dust from iron and steel plant, *Appl. Mech. Mater.*, 295-298(2013), p. 3075.